PHYSICAL REVIEW VOLUME 77, NUMBER 5 MARCH 1, 1950

Nuclear Cross Sections for 95-Mev Neutrons*

JAMES DEJUREN AND NORMAN KNABLE
Radiation Laboratory, Department of Physics, University of California, Berkeley, California
(Received November 18, 1949)

The total cross sections of twelve different elements were measured using the neutron beam from the 184-inch cyclotron operating with deuterons. Bismuth fission ionization chambers were employed as both monitor and detector in conventional "good geometry" attenuation measurements in the neutron flux emerging from the three-inch diameter collimating port in the 10-foot thick concrete shielding. The mean energy of detection of the neutrons in this experiment is estimated to be 95 Mev.

Measurements were also made with a monitor and detector placed inside the concrete shielding where we could obtain an intense neutron flux over a large area. Attenuators of four different elements were placed in front of the detector in a "poor geometry" arrangement so that attenuation was due essentially to inelastic collisions which degrade the neutron energy below the fission threshold. A second detector was placed outside the concrete shielding in the collimated neutron beam in line with the neutron source, absorber, and first detector. Attenuation in it is caused by both inelastic and elastic scattering. By this arrangement the ratio of inelastic to total cross section can be determined directly in one experiment.

The nuclear radii as calculated from the observed cross sections using the theory of the transparent nucleus vary as $1.38\times10^{-13}\,A^{\frac{1}{3}}$ cm. In this energy range the ratios of the inelastic to total cross sections are all less than one-half.

INTRODUCTION

SEVERAL experiments have been conducted to measure the cross sections of nuclei with neutrons. They have been spaced at intervals corresponding to the periods when an increase in the energy of the bombarding neutrons was made available. It was thought that as the available energies increased the measured cross sections would tend to become independent of the energy of the bombarding particle. The results of these previous measurements are summarized in a recent paper of Cook, McMillan, Peterson, and Sewell[1] which describes a measurement of cross sections using the neutrons produced by 190-Mev deuterons of the 184-inch cyclotron.

The threshold energy of the reaction used for detecting the neutrons $C^{12}(n,2n)C^{11}$, is 20 Mev and an average cross section is obtained for neutrons having the average energy of the distribution produced in the cyclotron, modified by the $(n,2n)$ cross-section energy dependence. This work showed the expected $A^{\frac{1}{3}}$ variation of the nuclear radius, calculated from an opaque nuclear model, for heavy nuclei but clearly indicated that the light nuclei (carbon and lighter) had smaller apparent radii than would be expected from an $A^{\frac{1}{3}}$ law. This effect was attributed to the transparency of the light nuclei for neutrons of short wave-lengths.

These results indicated the need for a similar experiment to be done at higher energies in order to investigate the energy dependence of the effect. The estimated average energy of detection in the early experiment was 83 Mev. In the experiment to be described, the same source of neutrons was employed, but a bismuth fission ionization chamber[2] with a threshold of about 50 Mev and a mean detection energy of 95 Mev served as the detector. In addition to raising the average detection energy this high threshold served a second purpose; it allowed us to measure the cross sections for inelastic processes.

Such a measurement was necessary for one could no longer assume that the cross sections for inelastic scattering and for elastic scattering were equal to each other and to one-half the total cross sections as would be expected from an opaque model of the nucleus. The nuclear transparency would cause the ratio of inelastic and elastic scattering cross sections to be energy dependent.

Fernbach, Serber, and Taylor[3] have, by assuming a model of the nucleus which has an absorption coefficient and an index of refraction, arrived at a formula for the radius of the nucleus in terms of the total cross section which for the experimental cross sections given shows the radii of the nuclei to be directly proportional to $A^{\frac{1}{3}}$ within the limits of experimental error. The same good fit has been made with the data of the previous experiment using the index of refraction and absorption coefficient corresponding to the neutron momentum of the average energy of detection in that experiment.

The total cross sections of 12 different nuclei are measured employing bismuth fission ionization chambers as both monitor and detector in conventional "good geometry" attenuation measurements in the neutron flux emerging from a three-inch diameter collimating port in the ten-feet thick concrete shielding.

Measurements were also made with a monitor and detector placed inside the concrete shielding where we could obtain an intense neutron flux over a large area. Attenuators of four different elements were placed in front of the detector so that the angle subtended by the attenuator was greater than the angle at which the differential scattering cross section of the attenuator nuclei falls to one percent of its value in the forward direction. This arrangement simulated the situation in which a plane wave of neutrons strikes a slab of material infinite in area so that attenuation is due solely to

* This work was performed under the auspices of the AEC.
[1] Cook, McMillan, Peterson, and Sewell, Phys. Rev. 75, 7 (1949).
[2] C. Wiegand, Rev. Sci. Inst. 19, 790 (1948).
[3] S. Fernbach, R. Serber, and T. B. Taylor, Phys. Rev. 75, 1352 (1949).

inelastic collisions. Measurements with higher threshold detectors gave results which agreed within the probable errors, thus confirming our assumption that an inelastic collision reduces the neutron energy below the threshold for bismuth fission.

A second detector was placed outside the concrete shielding in the collimated beam in line with the neutron source, attenuator, and first detector. Attenuation of the beam for the last detector is caused by both elastic and inelastic scattering. By this arrangement the ratio of inelastic to total cross sections can be measured directly in one experiment.

COUNTERS AND NEUTRON DETECTION

Counters

The ionization chambers[2] employed outside the concrete shielding contained 31 aluminum disks $\frac{1}{32}$-inch thick and two inches in diameter (Fig. 1). Alternate disks were coated with thin layers of bismuth and the separation between adjacent disks was $\frac{3}{8}$ inch. The disks of the chambers used as monitors were plated with bismuth 1.0 to 1.5 mg/cm^2 thick; the detector disks with bismuth 10 mg/cm^2 thick. For exposure to equal neutron flux the detector counting rate is three to four times that of the monitors. The chambers employed in the "poor geometry" measurements inside the shielding were of a shallow design, containing three plates 4.5 inches in diameter, $\frac{3}{4}$ inch apart. Thin bismuth layers were used (as in the monitors described). The fragments produced in fission of bismuth by the high energy neutrons experience their greatest rate of energy loss at the beginning of their ranges since they are initially multiply ionized and recombine with electrons as their velocities decrease. Hence most of the ionization in the argon gas occurs near the negative, bismuth coated plates. The electrons formed are collected on the aluminum plates (field strength 500 v/cm) and the resulting pulses are amplified by means of linear amplifiers.

Pulse Characteristics

The number of ions produced by a bismuth fission fragment is much greater than that by an alpha-particle or proton given off by a spallation reaction in the chamber. Consequently it will take coincidences of several spallation reactions to give a pulse as large as a fission pulse. The gas used in the chambers was argon with 3 percent carbon dioxide, and the pressure was adjusted so that the range of the fission fragments was approximately equal to the separation of the plates, since at a higher pressure the total ionization in the gas from a fission fragment would be unchanged but the ionization from an alpha-particle would increase proportionally with pressure. If at a given neutron intensity the logarithm of the counting rate is plotted against the discriminator voltage (Fig. 2) a curve with a broad plateau is obtained. The variation of the counting rate on the plateau is usually one to two percent, per volt change of discriminator voltage. If the logarithm of the ratio of the number of counts of the chamber to a fixed monitor is plotted against discriminator voltage a similar curve results. If the neutron intensity is increased, the rapidly varying "pile-up" region of the curve, due to pulses from coincident spallation reactions is shifted to the right, but the remainder of the curve is unchanged. This agrees with what we would expect from theoretical considerations, which show the number of "pile-ups" to be a much more rapidly increasing function of the neutron intensity than is the number of fissions. Variation of neutron intensity thus affords a criterion for distinguishing fission pulses from "pile-ups" of spallation products.

The stability of the amplification and discrimination voltages was periodically checked by feeding in fixed voltage pulses and it was determined that the experimental errors so incurred were less than the statistical errors of counting.

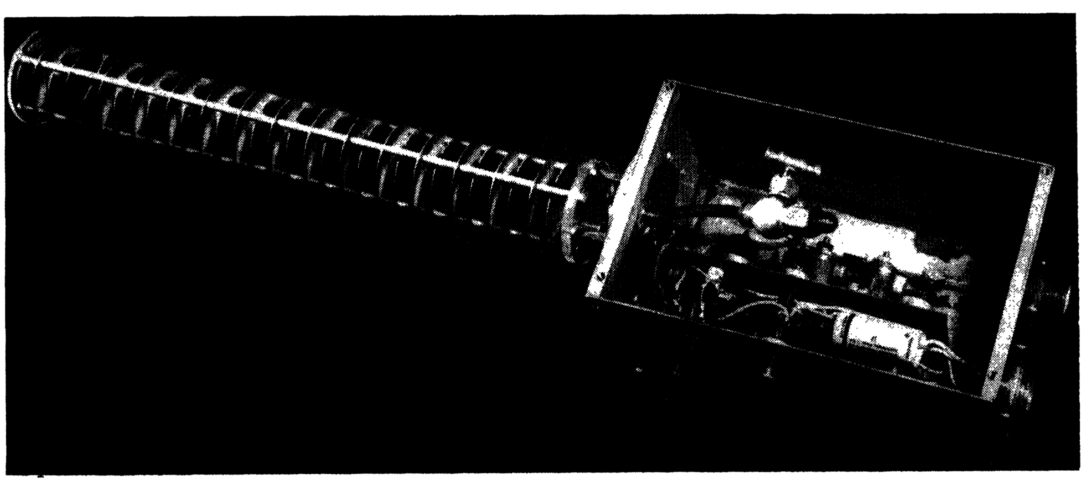

FIG. 1. Internal structure of long fission ionization chamber.

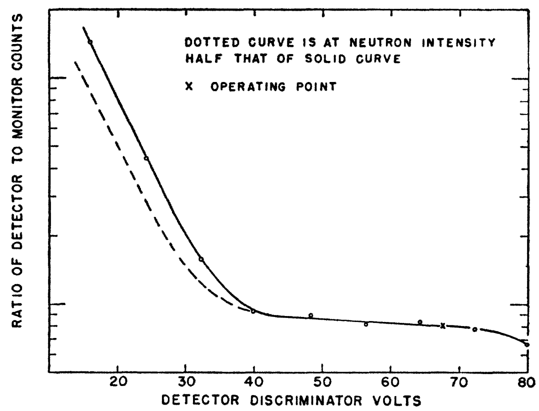

FIG. 2. Discriminator curve: Number of pulses greater than discriminator voltage *vs.* discriminator voltage.

EFFECTIVE NEUTRON DETECTION ENERGY

The neutron beam was produced by bombarding a 0.5-inch Be target with 190-Mev deuterons in the 184-inch cyclotron. The neutrons produced by "stripping" have an energy distribution theoretically predicted by Serber[4, 5] and checked experimentally with proton recoil counters[6] and by proton recoils in a cloud chamber.[7] The variation of the fission cross section with neutron energy was investigated by Wiegand and Kelly[8] by varying the radius of the target probe in the 184-inch cyclotron. As there is a spread in neutron energies for each radius and the more energetic neutrons in each energy spectrum have the highest fission efficiency, the curve of bismuth fission cross section as a function of neutron energy may be even steeper than indicated. If the fission cross section and neutron distribution for corresponding energy intervals are multiplied a curve results proportional to the detection efficiency as a function of neutron energy (Fig. 3). The curve is similar to the original neutron distribution; both curves have an energy spread of about 26 Mev at half-maximum, but the average energy of the neutrons detected by fission is about 95 Mev.

EXPERIMENTAL ARRANGEMENTS

Arrangement for Total Cross Sections

The monitors and detectors employed in measuring total cross sections were aligned outside the concrete shielding by means of x-ray film (which was exposed to γ-rays formed when deuterons struck the target). The attenuators were placed behind the monitor at a distance of 100 inches from the detector (Fig. 4), so that the detector subtended a solid angle of 0.0003 steradian at the attenuator. A steel collimator, 18 inches long with a 1-inch$\times$1.5-inch cross-sectional aperture placed in the collimating port through the shielding, was employed in all but the first few experiments. The correction for small angle scattering was negligible when the collimator was used, and the maximum correction without the collimator was only 2.2 percent for the Pb cross section.

Arrangement for Inelastic Cross Sections

The two shallow type chambers mentioned earlier were equipped with cathode followers that would function in the stray magnetic field inside the concrete shielding. These chambers could be placed in the broad neutron beam[5] outside the cyclotron tank. One chamber was placed in the central portion of the beam in line with the probe and collimator (Fig. 4). Absorber slabs could be placed in front of this chamber in "poor geometry" fashion. The second chamber was placed to one side of the absorbers to serve as a monitor (Fig. 5). The absorbers were stacked in a conical array as shown in Fig. 4. The angular distribution of elastically scattered neutrons from nuclei is peaked in the forward direction and even for carbon the fraction singly scattered more than 45° is negligible; so the conical half-angle of 45° employed, permitted essentially all the elastically scattered neutrons to enter the "poor geometry" detector that would have entered even if the slabs were infinite in area. The attenuation, therefore, is a measure of the cross section for inelastic collision.

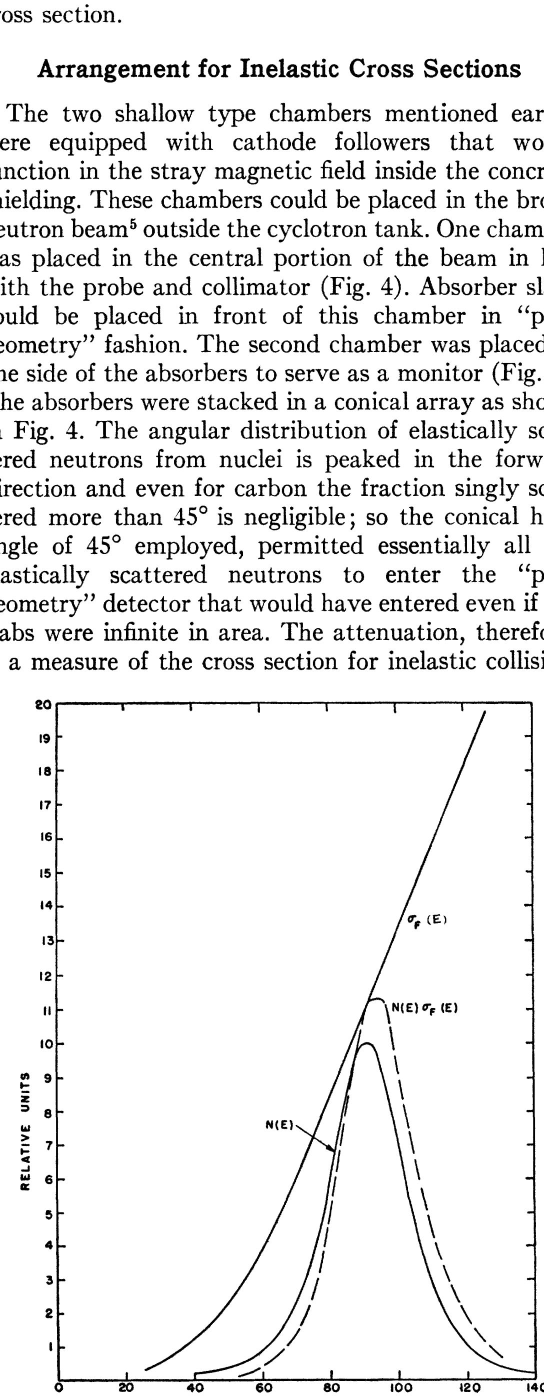

FIG. 3. $\sigma_f(E)$—fission cross section of bismuth, for neutrons $N(E)$—energy distribution of neutrons, and $N(E)\sigma_f(E)$—detection efficiency.

[4] R. Serber, Phys. Rev. **72**, 1008 (1947).
[5] A. C. Helmholz, E. McMillan, and D. Sewell, Phys. Rev. **72**, 1003 (1947).
[6] Hadley, Kelly, Leith, Segrè, Wiegand, and York, Phys. Rev. **75**, 357 (1949).
[7] Brueckner, Hartsough, Hayward, and Powell, Phys. Rev. **75**, 555 (1949).
[8] E. L. Kelly and C. Wiegand, Phys. Rev. **73**, 1135 (1948).

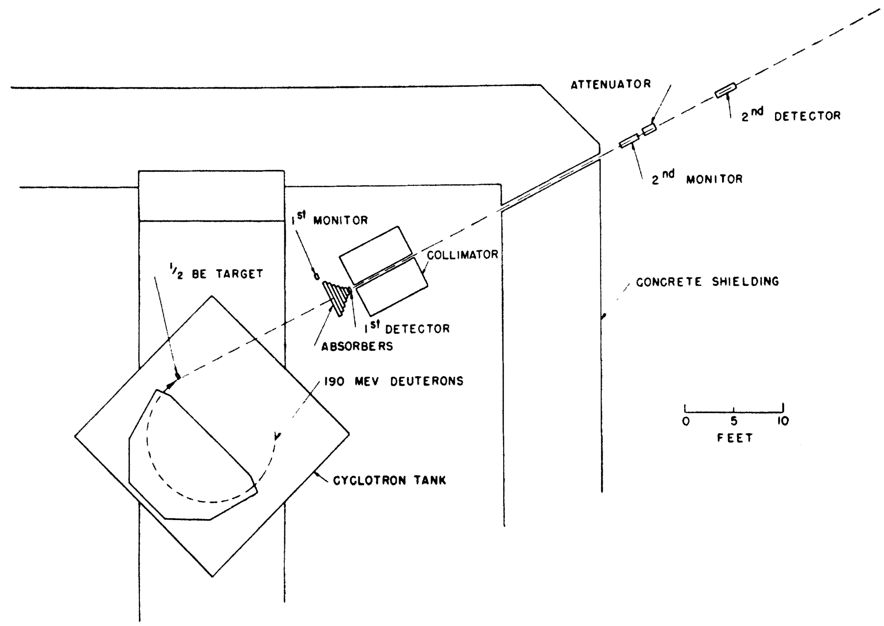

FIG. 4. Arrangement of apparatus.

A detector was also placed outside the shielding, as previously mentioned, in line with the collimated beam, so measurements of total and inelastic cross sections could be measured simultaneously.

The total thickness of attenuators used was restricted by the condition that the flux should be uniform over the first disk (largest in area). A survey of the uniformity was made by moving a shallow fission chamber with 2-inch diameter bismuth-coated plates over the region where the "poor geometry" attenuators were placed. The neutron flux was uniform (within 95 percent of the peak value) over an area 7 inches in radius. Disks greater than 8 inches in radius could not be used because the cyclotron deflector housing reduced the beam intensity at that radius. The attenuation was exponential over more than two inelastic mean free paths of copper, with no transition effects.

Magnitude of Attenuation Employed

As the attenuation was exponential, within the probable errors, for both the "good" and "bad" geometry experiments, it was not necessary to measure the slope of a semi-log plot of the intensity *versus* thickness (Fig. 6). Measurements were made with between one and two mean free paths of material.

For the experiments performed outside the shielding the monitor and detector counting rates were normally about equal with no attenuator present. The statistical error in the value of the cross section measured is equal to the statistical error of counting divided by the number of mean free paths of absorber. The principal counting error results from the detector reading with attenuator present. Slightly over two mean free paths of material was the most efficient length for a cross section determination, but to minimize diffraction scattering into the detector usually less than two mean free paths were employed.

ATTENUATOR MATERIALS

Physical Properties

The metals used in the experiments were usually machined cylinders and were measured by two different observers with micrometer or vernier calipers and carefully weighed. The liquids employed were weighed in a 500-ml volumetric flask, which was first calibrated

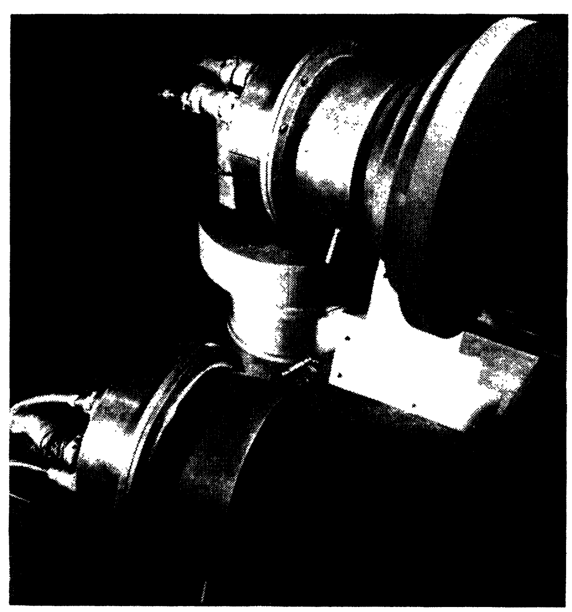

FIG. 5. Fission chambers and absorbers used in "poor geometry" measurements.

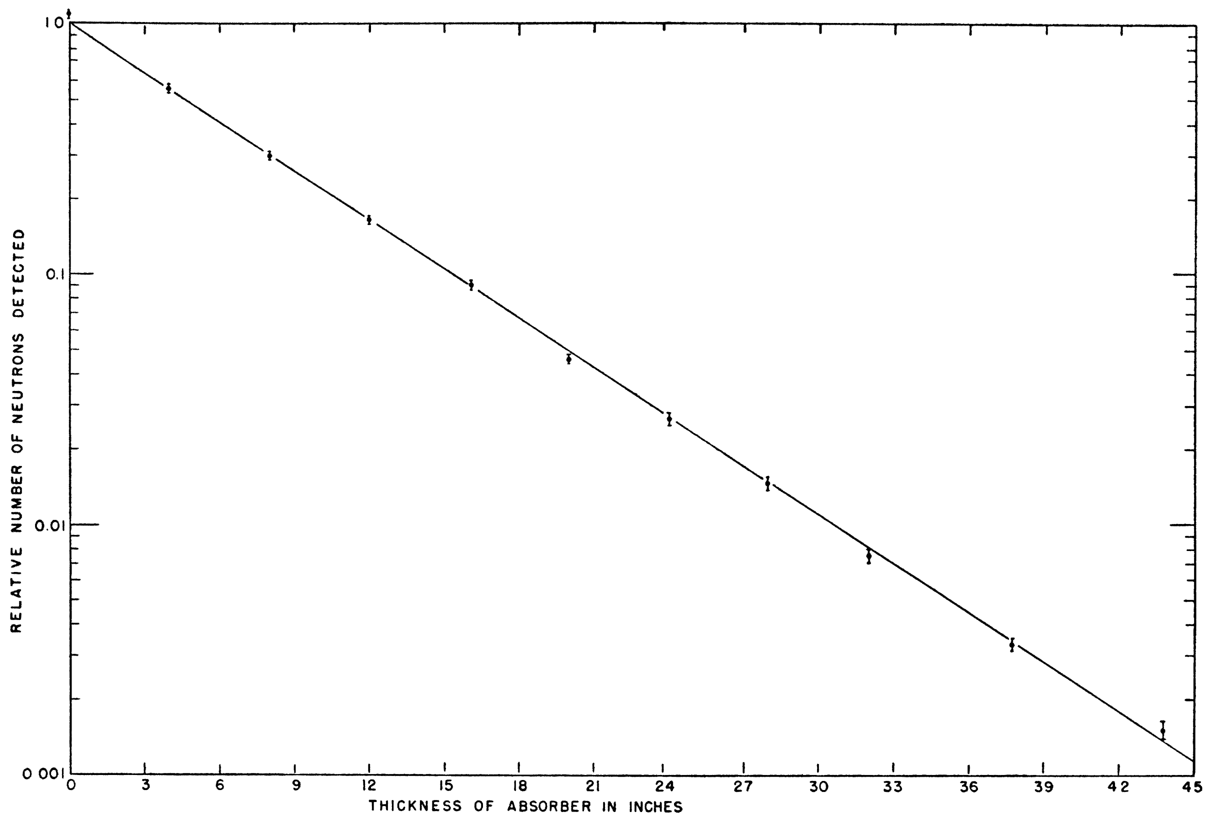

FIG. 6. Absorption of neutrons in Al.

by weighing distilled water at 19.1°. The measured value of the density was 0.9980 g/ml while the accepted value is 0.9984 g/ml.

The liquids were held in a 3-inch inner diameter cylindrical brass holder of variable length with $\frac{1}{16}$-inch thick brass end caps. During an experiment several counting intervals were employed with the holder alternately filled and empty.

The nitrogen cross section was derived from melamine, $C_3H_6N_6$. The melamine was carefully tamped in the brass holder in an effort to make the density as uniform as possible. An alternate empty holder with similar caps was employed during the "blank" counting intervals.

When the holder was used the beam from the 1-inch $\times$1.5-inch collimator was always carefully centered by means of x-ray film to minimize scattering from the brass walls.

Purity of Attenuators

Chemically pure materials were used, and the effect of minute impurities on the values obtained is negligible.

Because of its theoretical importance the total cross section of hydrogen was measured carefully on three separate occasions using pentane-carbon differences. Six graphite cylinders were machined to fit in the brass liquid holder. The length of the holder was adjusted (43 inches) so that the mass per unit area of carbon in the graphite was equal to the carbon in the pentane employed. The graphite cylinders were distributed along the length of the holder to simulate the distribution of carbon in the pentane. A counting interval was first taken with graphite in the holder. When the pentane was substituted the attenuation in the detector over the previous case was due solely to the hydrogen in the pentane. Hence the counting errors are due to these cycles only and the hydrogen cross section is directly obtained without the need of blank cycles, which would introduce added statistical errors. As only 0.5 mean free path of hydrogen was present and the statistical error of the cross section is the counting error divided by the mean free path, it was important to use the counting time efficiently.

The graphite and pentane were analyzed by the Pacific Chemical Laboratories for impurities which were as follows:

Sample	Impurities	Percentage
Graphite	Silicon	0.052
	Sulfur	0.067
	Iron	0.011
	Others	0.020
Pentane	Sulfur	0.045

The error introduced by these impurities is not significant.

The difference between the deuterium and hydrogen cross sections was determined directly in a similar experiment by filling the holder alternately with equal numbers of D_2O and H_2O molecules. The heavy water was 99.87 percent D_2O by weight.

RESULTS

Total Cross Sections

The data for the total cross sections measured outside the shielding are given in Table I. Corrections for diffraction scattering are included in a few cases where this is significant. Statistical errors given are in terms of standard deviations. The effect of background was investigated by placing fourteen mean free paths of various absorbers between detector and monitor. Without absorbers 950 detector counts were obtained for 1000 monitor counts. With absorbers no detector counts were obtained for 3600 monitor counts. Even a few detector counts would have meant negligible error from background. As the chambers have excellent high-voltage and discriminator characteristics, the error introduced by the equipment is probably less than one percent. Repeated measurements have given differences that appear to be purely statistical.

TABLE I. Total cross sections for 95-Mev neutrons measured with bismuth fission chambers.*

Element	Density g/cm^3	Atomic number Z	Mass number A	$A^{1/3}$	Cross section $\sigma_t \times 10^{24}$ cm^2	Radius, $R \times 10^{13}$ cm from model
Hydrogen		1	1	1.00	0.0745±0.002	1.69±0.02
					0.073 ±0.003	
					0.071 ±0.002	
					0.073 ±0.0015 (ave.)	
Deuterium		1	2	1.26	0.104 ±0.004	1.89±0.03
Beryllium	1.847	4	9	2.08	0.396 ±0.004	2.94±0.015
Carbon	1.580	6	12	2.29	0.502 ±0.004	3.20±0.01
					0.502 ±0.005	
					0.490 ±0.004	
					0.494 ±0.004	
					0.501 ±0.006	
					0.498 ±0.003 (ave.)	
Nitrogen		7	14	2.41	0.570 ±0.007	3.35±0.02
Oxygen		8	16	2.52	0.663 ±0.007	3.52±0.02
Aluminum	2.714	13	27	3.00	0.993 ±0.011	4.11±0.02
Chlorine		17	35.46	3.29	1.28 ±0.02	4.55±0.03
Copper	8.90	29	63.57	3.99	2.00 ±0.02	5.53±0.03
					2.00 ±0.03	
Tin	7.28	50	118.7	4.92	3.18 ±0.03	6.81±0.03
					(3.13)	
Lead	11.33	82	207.2	5.92	4.48 ±0.03	8.14±0.03
					(4.38)	
Uranium	18.89	92	238.1	6.20	4.92 ±0.06	8.58±0.05
					(4.89)	
Deuterium-Hydrogen Compounds		0	1	1.00	0.031 ±0.002	
H_2O	0.998				0.815 ±0.005	
					0.807 ±0.005	
D_2O	1.104				0.868 ±0.005	
Pentane C_5H_{12}	0.627				3.40 ±0.03	
					3.37 ±0.03	
					3.32 ±0.02	
CCl_4	1.592				5.61 ±0.07	
Melamine $C_3H_6N_6$					5.37 ±0.035	

* Values in parentheses are not corrected for diffraction scattering.

TABLE II. Inelastic cross sections for 95-Mev neutrons measured with bismuth fission chambers.

Element	σ_i/σ_t	$\sigma_t \times 10^{24}$ cm^2	Total M.F.P. used
Carbon	0.460±0.016	0.496±0.012	0.60
	0.457±0.026	0.489±0.018	
	0.434±0.023	0.497±0.017	
	0.431±0.024	0.498±0.017	
	0.454±0.022	0.502±0.016	
Aluminum	0.42 ±0.015	0.995±0.02	0.94 (Dural)
Copper	0.39 ±0.005	2.005±0.02	2.5
Lead	0.40 ±0.01	4.46 ±0.06	1.9
	0.38 ±0.01	4.46 ±0.06	
	0.40 ±0.01		
Carbon (ave.)	0.45 ±0.015	0.497±0.008	

Inelastic Cross Sections

The inelastic cross-section measurements are subject to greater sources of error. The "poor geometry" detectors count inelastically scattered neutrons or neutrons ejected from nuclei if their energies are above the threshold for bismuth fission. The inelastic cross sections obtained, therefore, represent a lower limit to the true values. However, it is not expected that the contribution of neutrons over threshold energy from inelastic processes is large enough to modify the present interpretations.

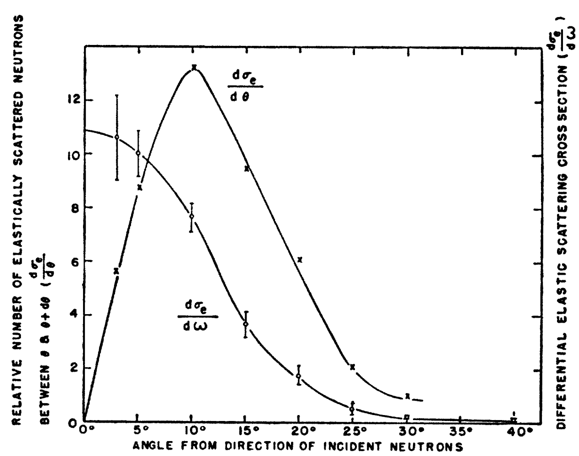

FIG. 7. Angular distribution of elastically scattered neutrons from carbon.

Elastically scattered neutrons will have a greater path length than undeviated neutrons in both the absorber and the bismuth layer of the detector. The relative probability of detection for different neutron paths is discussed in the appendix. Table II contains the experimental results. The ratio of σ_i/σ_t is given, since it is independent of density determinations of the material used and is measured directly. The total cross sections listed in Table II were measured with "better" geometry than those in Table I, and therefore require no corrections for diffraction. Actually dural was used,

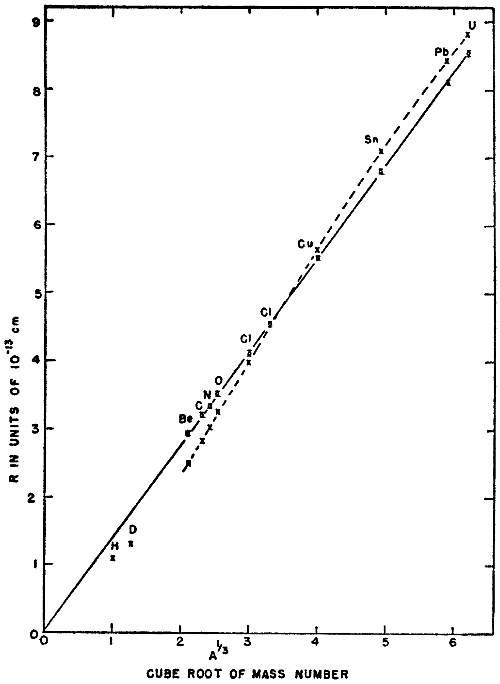

FIG. 8. Radii calculated from model assuming $K=3.00\times10^{12}$ cm^{-1} and $k_1=2.85\times10^{12}$ cm^{-1} define straight line of Eq. $R=1.38\times A^{\frac{1}{3}}\times10^{-13}$ cm. Dotted line is graph of radii calculated from $\sigma_t=2\pi R^2$ (opaque nucleus).

instead of aluminum, but the correction for the impurities (mainly copper) is negligible for the ratio of σ_i/σ_t.

An attempt was made to measure the ratio of σ_i/σ_t for carbon and copper using gold fission for neutron detection, since gold presumably has a higher fission threshold than bismuth. The values obtained were:

Element	σ_i/σ_t	σ_t
Carbon	0.42 ± 0.04	0.48 ± 0.35
Copper	0.38 ± 0.015	1.92 ± 0.06

The counting rate was about a factor of ten less for gold fission than for bismuth. From the total cross sections obtained, the average energy of neutrons detected is estimated to be between 100 and 105 Mev. Evidently the use of a higher threshold did not observably increase the ratio of σ_i/σ_t above the bismuth fission values. Both methods of detection agree, within the statistical errors.

An experiment was made to determine the angular distribution of elastically scattered neutrons from a carbon sphere. A fission chamber mounted on a radial arm pivoted below the sphere was used as the detector. The distribution is plotted in Fig. 7.

DISCUSSION OF RESULTS

The Transparent Nucleus Model

Fernbach, Serber, and Taylor[3] in a recent paper, have assumed a model for nuclei bombarded by high energy neutrons, in which the nucleus is regarded as a sphere of material characterized by an absorption coefficient and index of refraction, both of which are functions of the neutron momentum. Using their notation, k_1 is the increase of the propagation vector of the neutron wave upon entering the nucleus and K is the absorption coefficient. A wave going a distance x in nuclear matter will have its amplitude and relative phase changed by a factor $e^{(-\frac{1}{2}K+ik_1)x}$. The solutions for the inelastic and elastic cross sections are respectively:

$$\sigma_i=\pi R^2\left\{1-\frac{1-(1+2KR)e^{-2KR}}{2K^2R^2}\right\},$$

$$\sigma_e=2\pi\int_0^R |1-e^{(-K+2ik_1)s}|^2 s ds.$$

The form for σ_e is merely indicated, as the integrated expression is quite complex. R is the radius of the nucleus and $\sigma_t=\sigma_i+\sigma_e$.

Taylor has determined $k_1=2.85\times10^{12}$ cm^{-1} and $K=3.0\times10^{12}$ cm^{-1} to give the best straight line fit for the radii calculated from the total cross sections when R is plotted as a function of $A^{\frac{1}{3}}$. The equation for the line of best fit is $R=1.38A^{\frac{1}{3}}\times10^{-13}$ cm (Fig. 8).

The ratio of σ_i/σ_t for the afore-mentioned values of K and k_1 is given as a function of KR in Fig. 9 and the experimental values are shown.

Comparison with Data at 83 Mev

Cook, McMillan, Peterson, and Sewell[1] have measured total cross sections of the same elements in this laboratory using carbon disks, which have a 20-Mev threshold for the $C^{12}(n,2n)C^{11}$ reaction, for detectors. The average energy of the neutrons detected in their experiments is estimated to be 83 Mev as compared to 95 Mev for bismuth fission. The 95-Mev cross sections are roughly 10 percent smaller than those derived using carbon disks, indicating greater transparency at the higher energy.

ACKNOWLEDGMENTS

The authors wish to express their gratitude to Dr. Burton J. Moyer for his help and suggestions in car-

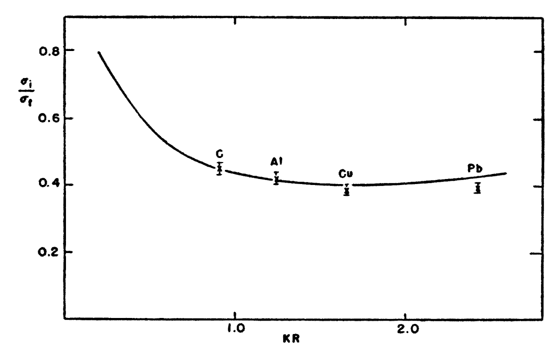

FIG. 9. Theoretical curve of σ_i/σ_t for $K=3.00\times10^{12}$ cm^{-1} and $k_1=2.85\times10^{-12}$ cm^{-1} with experimental points.

rying out the program, to the cyclotron crew for their cooperation in performing the experiments, and to Dr. E. Segrè, E. Kelly, and C. Wiegand for use of their vacuum evaporator for plating the chamber disks with bismuth and gold.

APPENDIX

Effect of Path Length on Inelastic Cross-Section Measurements

If I_0 be the number of neutrons/cm^2 on a plane absorber of thickness L, the number of neutrons/cm^2 suffering p elastic scattering events in traversing the material is given by:

$$I_{pL}=I_0\left(\frac{L}{\lambda_e}\right)^p\frac{1}{p.}e^{-L/\lambda_t}, \tag{A}$$

where λ_e and λ_t are the mean free paths for elastic scattering, and for any type of collision, respectively.

If $[d\sigma_e(\theta)]/d\omega$ is the differential cross section per unit solid angle for elastic scattering at angle θ, the number of neutrons/cm^2 emerging with angles between θ and $\theta+d\theta$ with respect to the incident neutrons is:

$$dI(\theta)=I_0\sum_{p=1}^{\infty}\left(\frac{L}{\lambda_e}\right)^p\frac{1}{p!}e^{-L/\lambda_t}\frac{1}{p}\frac{d\sigma_e(\theta/(p)^{\frac{1}{2}})}{d\omega}\frac{2\pi\sin\theta d\theta}{\sigma_e}$$

$$=\sum_{p=1}^{\infty}I_{pL}\frac{1}{p}\frac{d\sigma_e(\theta/(p)^{\frac{1}{2}})}{d\omega}\frac{2\pi\sin\theta d\theta}{\sigma_e}, \tag{B}$$

where it has been assumed that the effect of p elastic scatterings on the angular distribution is to broaden the distribution by a factor of $(p)^{\frac{1}{2}}$, and to decrease its height by $1/p$. Formulas A and B are only approximate since the path length is equal to L for small angles only.

The probability of a neutron emerging at angle θ, after sustaining an elastic collision into the θ direction within an element dx at depth x, is:

$$e^{-x/\lambda_t}\frac{dx}{\lambda_e}\cdot\exp\left[-\left(\frac{L-x}{\lambda_t\cos\theta}\right)\right].$$

The average attenuation experienced by neutrons following such a path is, from the above expression:

$$\frac{1}{L}\int_0^L\exp\left[-\frac{1}{\lambda_t}\left(x+\frac{L-x}{\cos\theta}\right)\right]dx.$$

The ratio of this attenuation at angle θ to the attenuation when $\theta=0$ is the relative probability of emergence for a neutron at angle θ compared with $\theta=0$.

After integrating, the result is

$$R_A=\frac{\lambda_t}{L}\frac{\cos\theta}{1-\cos\theta}\left\{1-\exp\left[\frac{-L}{\lambda_t}\left(\frac{1}{\cos\theta}-1\right)\right]\right\}.$$

The chance of a neutron inducing fission in the bismuth layer is proportional to its path length in the layer or to $1/\cos\theta$ since the chamber plates are normal to the undeviated neutrons.

In an elastic scattering event in the attenuator the scattered neutron will lose an amount of energy given by

$$\Delta E=\frac{2mE(1-\cos\theta)}{M+m(1-\cos\theta)},$$

where m is the neutron mass, M is the mass of the nucleus and E is the energy of the incident particle. Since the fission cross section is a function of energy the relative chance of producing a fission is

$$\sigma_f(E-\Delta E)/\sigma_f(E).$$

The probability of detecting a neutron scattered through angle θ relative to the probability of detecting an undeflected neutron is the product of the above factors for probability of emergence and probability of producing fission.

$$\frac{\pi_\theta}{\pi_0}=\frac{1-\exp[-n_t(1-\cos\theta)/\cos\theta]}{n_t(1-\cos\theta)}\frac{\sigma_f(E-\Delta E)}{\sigma_f(E)}, \tag{C}$$

where $n_t=L/\lambda_t$, the number of total mean free paths of attenuator.

The change in the bismuth fission cross section is given approximately by

$$d\sigma_f/\sigma_f=9/4(dE/E)$$

in the region of 90 Mev.

In our "poor geometry" experiments either n_t was small or the average angle of deviation was small (due to forward peaking of elastically scattered particles from heavy nuclei); so the exponent in Eq. (C) may be expanded:

$$\frac{\pi_\theta}{\pi_0}=\frac{1-[1-n_t(1-\cos\theta)/\cos\theta+n_t^2/2(1-\cos\theta)^2/\cos^2\theta+\cdots]}{n_t(1-\cos\theta)}\frac{\sigma_f(E-\Delta E)}{\sigma_f(E)}$$

$$\cong\left[\frac{1}{\cos\theta}-\frac{n_t(1-\cos\theta)}{2\cos^2\theta}\right]\frac{\sigma_f(E-\Delta E)}{\sigma_f(E)}. \tag{C$'$}$$

If we know the angular distribution of elastically scattered neutrons we can correct the inelastic cross section data using C$'$. For carbon the relative angular distribution of scattered neutrons in the annular region between θ and $\theta+d\theta$ is shown in Fig. 7. If the latter curve is multiplied by C$'$ which has been evaluated for carbon, the area under the curve increases by about 1.2 percent. Hence the number of singly scattered neutrons detected in the "poor geometry" experiment was increased by 1.2 percent due to the increased probability of detection for $\theta>0°$.

From A with $(L/\lambda_e)=0.33$ the relative number of neutrons emerging that were elastically scattered p times may be determined:

$p=0$: 71 percent
$p=1$: 25 percent
$p=2$: 4 percent.

Those scattered once and twice will have a greater probability of detection and the increase on the total number of detector counts was roughly 0.25×1.2 percent $+0.04\times 1.5$ percent (allowing a greater correction for double scattering) or 0.36 percent. This increase in the detector counts caused the inelastic cross section to be low by the increase divided by the number of inelastic mean free paths, 0.36/0.27 percent, or about 1.3 percent. Since the statistical error is 3.3 percent this correction is hardly significant.

The correction for the heavier nuclei is less, due to the greater forward peaking of the elastically scattered neutrons.

PHYSICAL REVIEW VOLUME 77, NUMBER 5 MARCH 1, 1950

Neutron-Deficient Cesium Isotopes*

RICHARD W. FINK, FREDERICK L. REYNOLDS, AND D. H. TEMPLETON
Department of Chemistry and Chemical Engineering and Radiation Laboratory, University of California, Berkeley, California
(Received October 31, 1949)

The new isotopes Cs^{127} and Cs^{129} have been produced from iodine by irradiation with high energy helium ions. Their mass assignments were determined with a mass spectrograph. Cs^{127} decays with 5.5 ± 0.5 hr. half-life with emission of positrons (1.2 Mev maximum energy), giving rise to the daughter activity 34-day Xe^{127}. Cs^{129} decays by electron capture with half-life 31 ± 1 hr. A 30-min. activity, presumed to be Cs^{130}, was also produced, but its mass assignment is uncertain.

THE successful completion of a thermally ionizing mass spectrograph in this laboratory and the availability of high energy helium ions from the Berkeley 184-in. cyclotron have led us to investigate neutron-deficient isotopes of alkali metals, which are relatively easy to ionize. Some results for rubidium isotopes have already been reported.[1] This paper is concerned with two new cesium isotopes.

The cesium isotopes of mass 131 and greater have been studied extensively.[2] The only report of lighter isotopes seems to be a 30-min. period produced from iodine with helium ions, presumably of 16 Mev energy from the Purdue University cyclotron.[3]

IODINE BOMBARDMENTS

Stable I^{127} (100 percent abundance) was bombarded in the form of ammonium iodide with 60-Mev helium ions in the Berkeley 184-in. cyclotron for periods of from one to four hours. The ammonium iodide was wrapped in 0.001-in. aluminum foil and irradiated mounted on a water-cooled copper block on the cyclotron probe. Elemental iodine sealed in a platinum capsule was also bombarded. Ammonium iodide was also bombarded with 36-Mev helium ions from the Crocker 60-in. cyclotron.

The cesium radioactivities induced were isolated from the target material by chemical procedures[4] designed to remove Xe, I, Te, Sb, Sn, and most other elements except alkali metals. Carrier cesium was added in some cases, but it was found that very little could be tolerated in samples destined for the mass spectrograph. It was found that sufficient Cs^{133} to serve as a reference line on the mass spectrum was provided

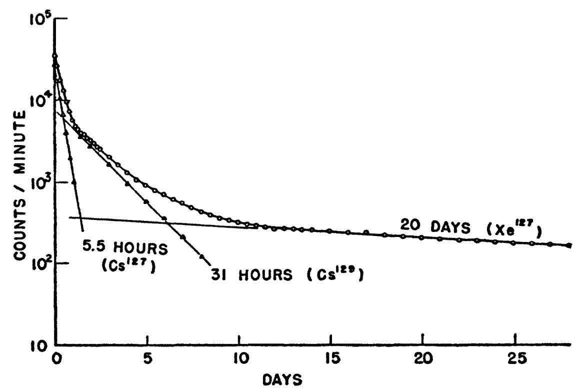

FIG. 1. Decay curve of cesium radioactivities induced by 60-Mev helium ions from ammonium iodide. The points at high counting rates were derived from data obtained at a lower geometry.

* This work was supported by the AEC.

[1] Reynolds, Karraker, and Templeton, Phys. Rev. **75**, 313 (1949).

[2] For references, see G. T. Seaborg and I. Perlman, "Table of isotopes," Rev. Mod. Phys. **20**, 585 (1948); also, Yaffe, Kirsch, Standil, and Grunlund, Phys. Rev. **75**, 699 (1949); N. Sugarman, Phys. Rev. **75**, 1473 (1949); J. L. Meem and F. Maienschein, Phys. Rev. **76**, 328 (1949); and J. S. Osoba, Phys. Rev. **76**, 345 (1949). The assignment of the 10-day cesium to mass 131 has now been confirmed with the mass spectrograph by Karraker, Reynolds, and Templeton, UCRL Report-285 (February 11, 1949) (to be published).

[3] "J. R. Risser and R. N. Smith, private communication from K. Lark-Horowitz," quoted from G. T. Seaborg and I. Perlman, reference 2.

[4] For details, see R. W. Fink, M.S. thesis, University of California, Berkeley, 1949.

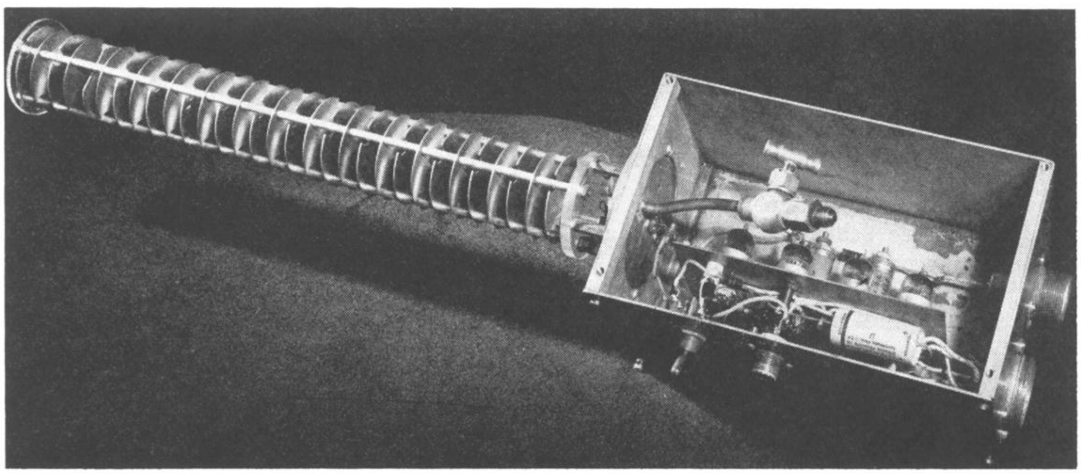

FIG. 1. Internal structure of long fission ionization chamber.

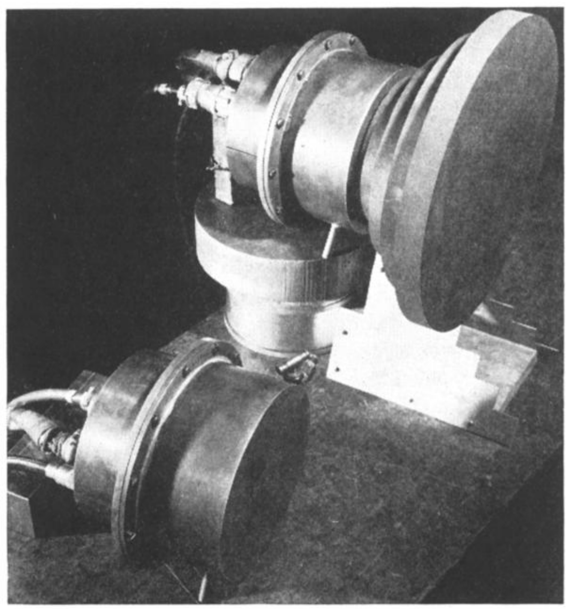

Fig. 5. Fission chambers and absorbers used in "poor geometry" measurements.